

## Supporting information

### A dimeric chlorite dismutase exhibits O<sub>2</sub>-generating activity and acts as a chlorite antioxidant in *Klebsiella pneumoniae* MGH 78578

Arianna I. Celis,<sup>1</sup> Zachary Geeraerts,<sup>2</sup> David Ngmenterebo,<sup>3</sup> Melodie M. Machovina,<sup>1</sup> Richard C. Kurker,<sup>4</sup> Kumar Rajakumar,<sup>3</sup> Anabella Ivancich,<sup>5</sup> Kenton R. Rodgers,<sup>2</sup> Gudrun S. Lukat-Rodgers,<sup>2,\*</sup> Jennifer L. DuBois<sup>1,\*</sup>

<sup>1</sup>Department of Chemistry and Biochemistry, Montana State University, Bozeman, MT 59715, USA

<sup>2</sup>Department of Chemistry and Biochemistry, North Dakota State University, Fargo, North Dakota 58102, USA

<sup>3</sup>Department of Chemistry and Biochemistry, University of Notre Dame, Notre Dame, IN 46556 USA

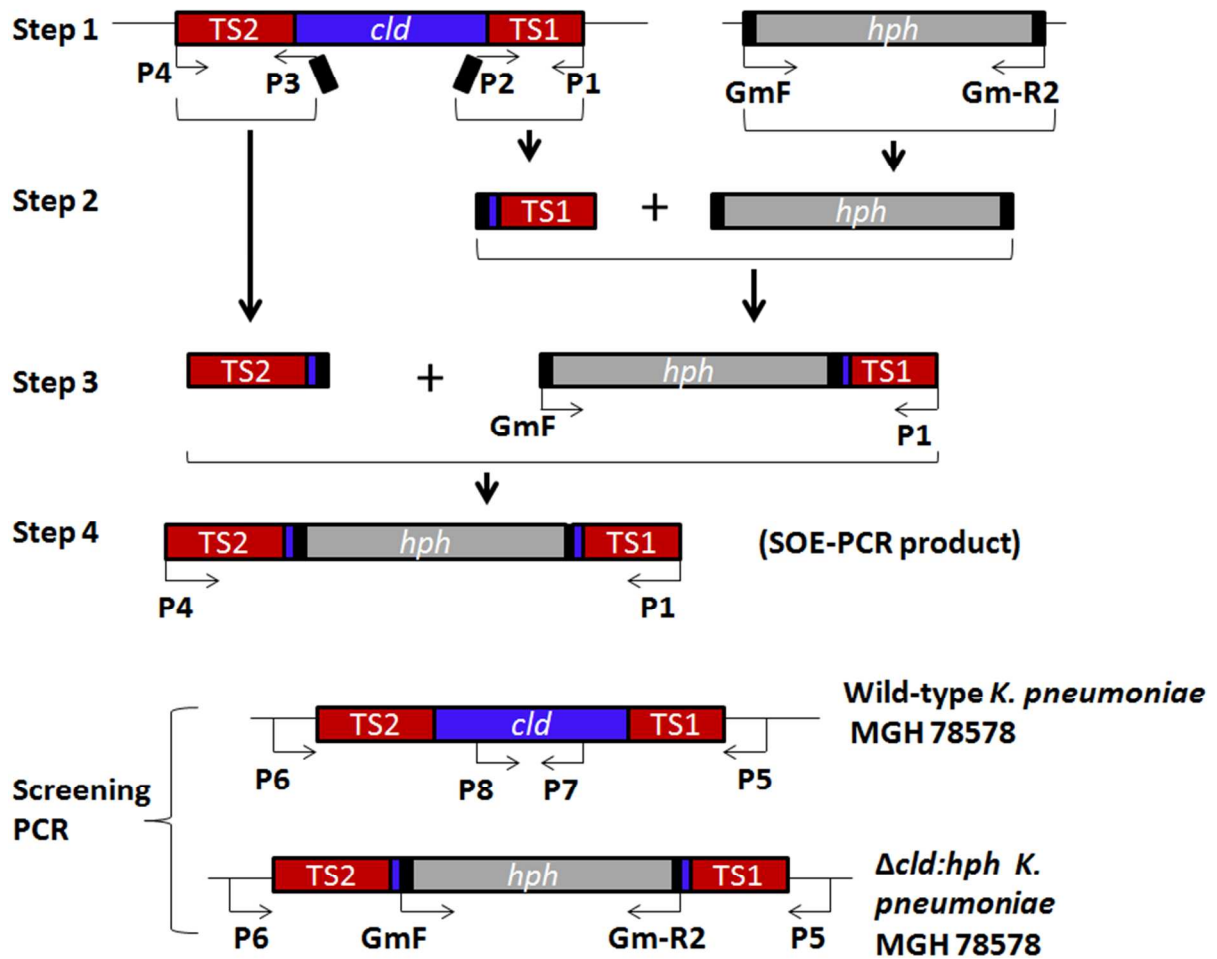
<sup>4</sup>Department of Infection, Immunity and Inflammation, University of Leicester, Leicester LE1 9HN, UK

<sup>5</sup>CNRS, Unité de Recherche Mixte CNRS/CEA/Université Paris-Sud (UMR 8221), Laboratoire de Bioénergétique, Métalloprotéines et Stress. Centre d'Etudes de Saclay, iBiTec-S, 91191 Gif-sur-Yvette, France

#### Contents:

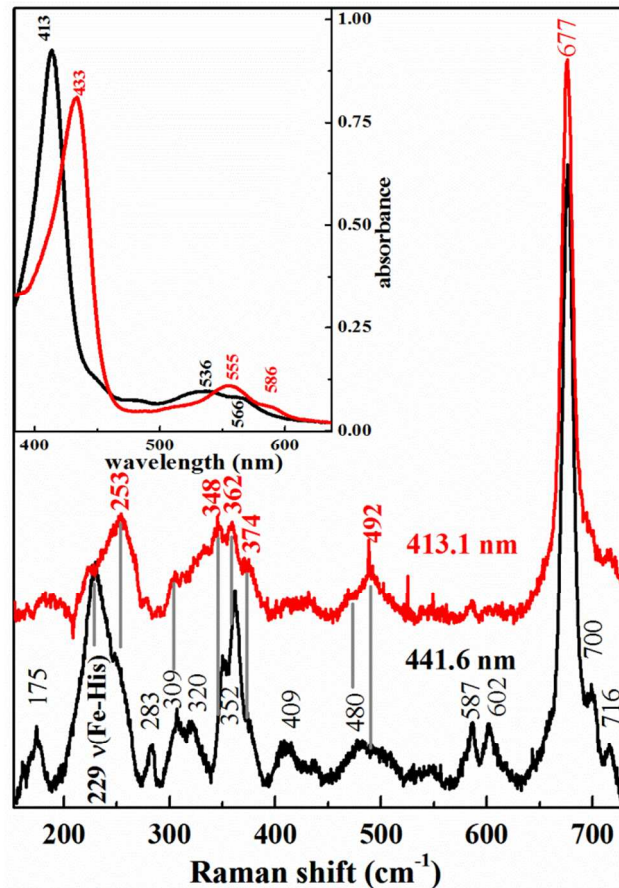
1. Figure S1. Schematic outlining the SOE-PCR and PCR validation strategy used to generate the  $\Delta cld$  strain.
2. Figure S2. Resonance Raman spectra for ferrous *KpCld*
3. Figure S3. Temperature dependent resonance Raman spectra
4. Figure S4. Steady state kinetic pH-rate profiles for the *KpCld* reaction with chlorite
5. Figure S5. Titration of *KpCld* heme spectrum with NaClO
6. Figure S6. Kinetics of the reaction between *KpCld* and NaClO at pH 6 and 8
7. Figure S7. Reactions of *DaCld* with ClO<sub>2</sub><sup>-</sup> in the presence/absence of MCD
8. Table S1. Bacterial strains and plasmids used in this study
9. Table S2. Oligonucleotide primers used in this study

**Figure S1.**



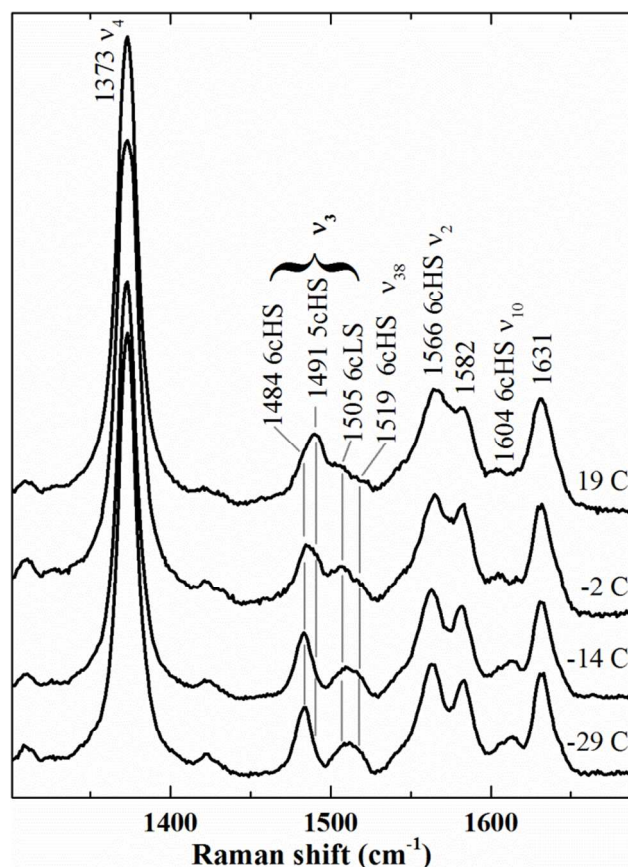
**Figure S1.** Schematic outlining the SOE-PCR and PCR validation strategy used to generate the  $\Delta cld$  strain. See text for further details.

**Figure S2.**



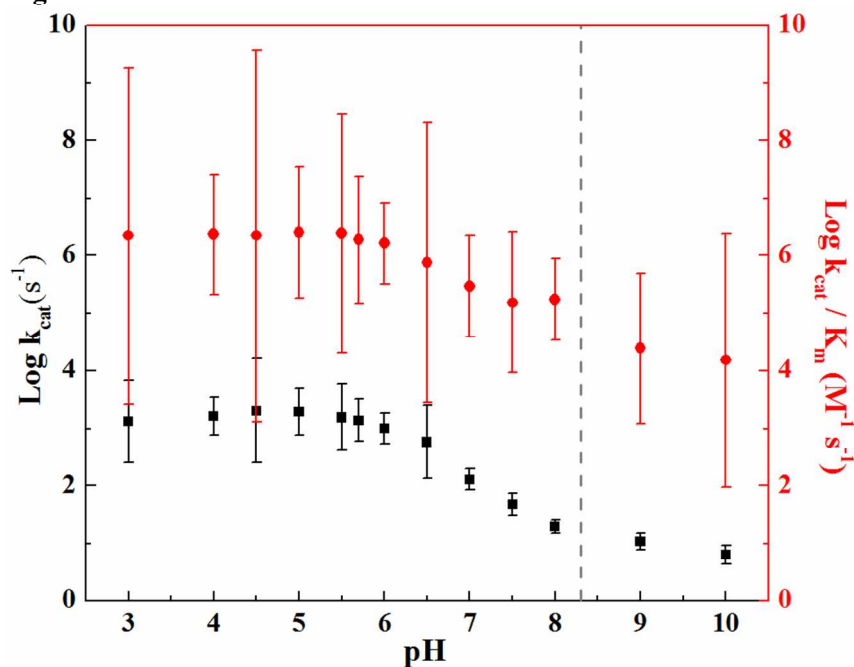
**Figure S2. The iron histidine stretch of ferrous *KpCld* is resonance enhanced with 441.6 nm excitation.** Comparison of rR spectra of ferrous *KpCld* pH 7.0 with 413.1 (red) and 441.6 nm (black) excitation. Inset: UV-visible spectra of ferric (black) and ferrous (red) *KpCld* pH 7.0 in 100 mM potassium phosphate buffer.

**Figure S3.**



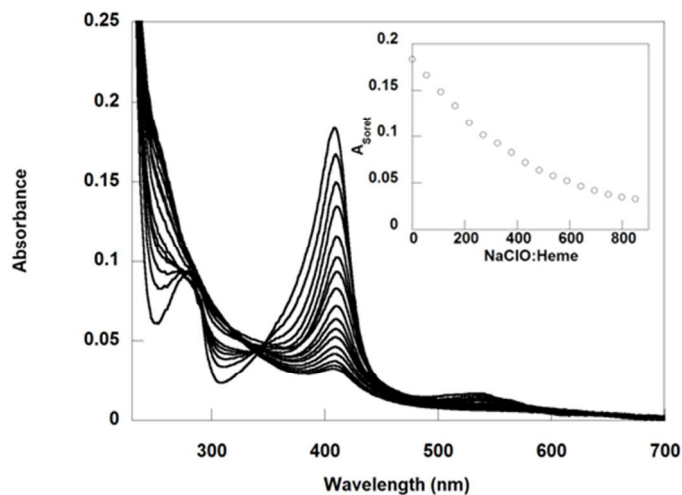
**Figure S3. Temperature dependence of the rR spectrum of ferric *KpCld* pH 6.0 indicates exothermic binding of water to the heme.** The high frequency rR spectra of ferric *KpCld* in 100 mM potassium phosphate pH 6.0 at the indicated temperatures were acquired with 413.1 nm excitation and 4 mW power at the sample. Temperature was controlled with a liquid N<sub>2</sub> boil off system. As the temperature is decreased, the broad  $\nu_3$  envelop encompassing contributions from 5cHS and 6cHS heme species sharpens to a symmetrical band consistent with a 6cHS aqua *KpCld* complex. As the 6cHS grows in, as judged by sharpening to the  $\nu_3$  band,  $\nu_{38}$  associated with this 6cHS complex also becomes prominent and overlaps with the  $\nu_3$  that suggests a small amount of 6cLS species at room temperature. Band assignments were made by analogy to metMb.

Figure S4.



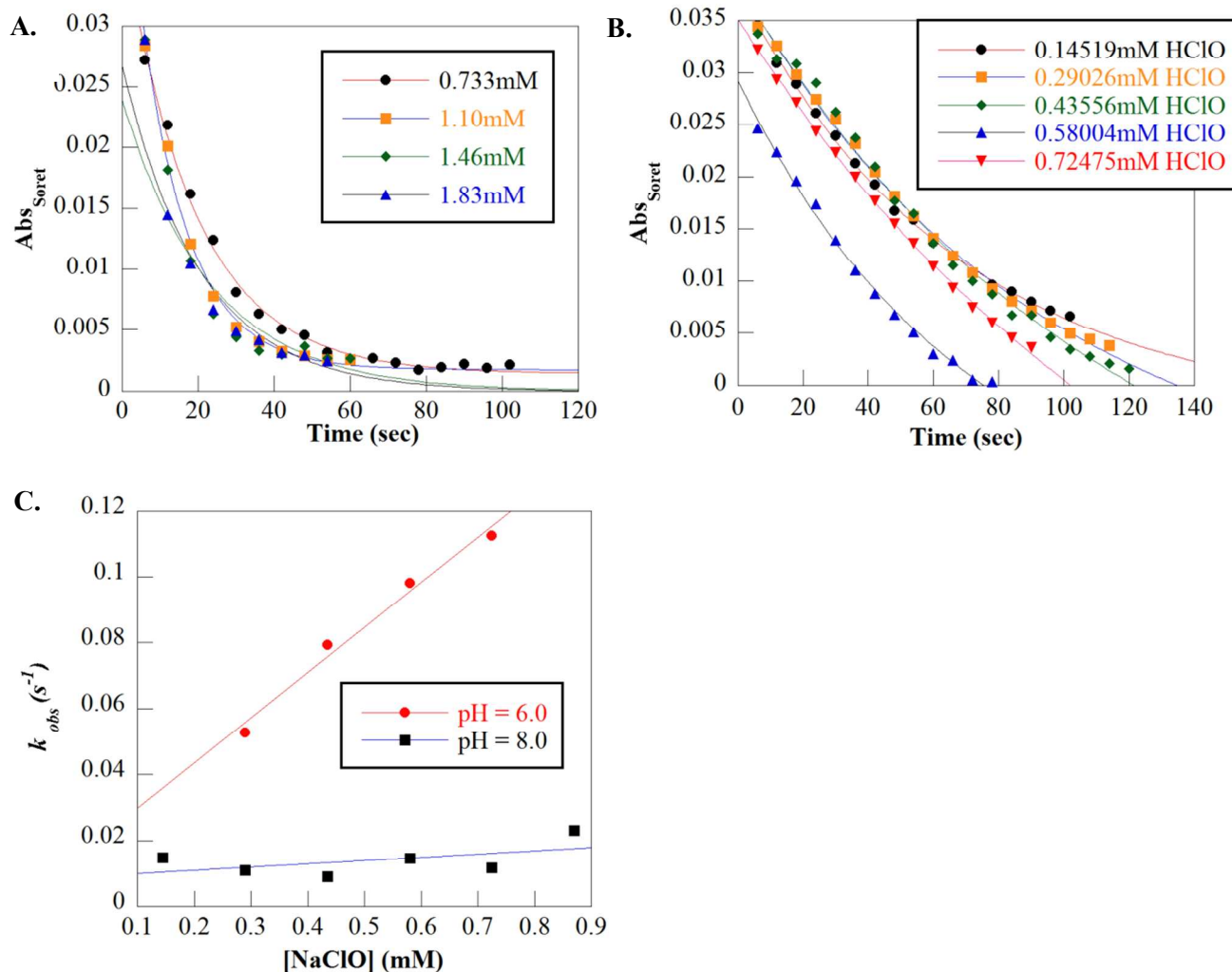
**Figure S4. Plots of the  $\log(k_{cat})$  (black squares) and the  $\log(k_{cat}/K_m)$  (red circles) for the chlorite decomposition reaction as a function of pH.** Initial rates of chlorite-decomposing activity in the steady state were measured with a luminescence based probe used to measure  $O_2$  evolution by *KpCld*. Samples were 12 nM WT *KpCld* and 0.05 – 2 mM chlorite in the following buffer solutions: 50 mM phosphate-citrate (pH < 6), 100 mM phosphate (pH 6-8), or glycine (pH > 8). Plots of  $\log(k_{cat})$  and the  $\log(k_{cat}/K_m)$  both show a single clear turning point corresponding to a  $pK_a$  of 7.0. This enzyme-localized (as opposed to heme-localized) deprotonation event decreases the enzyme activity and efficiency. The optimum activity is observed near pH 5.0 where  $k_{cat}$  and  $k_{cat}/K_M$  have values of  $1.9 (\pm 0.2) \times 10^3 s^{-1}$  and  $2.5 \pm (0.4) \times 10^6 M^{-1} s^{-1}$ , respectively. Above the enzyme-localized  $pK_a$ ,  $k_{cat}$  and  $k_{cat}/K_M$  drop to  $1.1 (\pm 1.6) \times 10^1 s^{-1}$  and  $2.4 \pm (0.7) \times 10^4 M^{-1} s^{-1}$  (pH 9.0), respectively.

**Figure S5.**



**Figure S5. Titration of *KpCld* heme spectrum with NaClO.** 50 $\mu$ L of 7.3  $\mu$ M heme-bound *KpCld* was added to 950 $\mu$ L citrate-phosphate buffer (50 mM, pH 6.0, room temperature ) in a UV/vis cuvette. A defined concentration of sodium hypochlorite was added and the solution was rapidly mixed. (Shown here is 0.90 mM an amount sufficient to nearly eliminate the heme Soret band. Several concentrations of NaClO were examined.) Spectra were scanned every 6s until the Soret band no longer changed. The inset shows the final Soret band absorbance plotted versus increasing [NaClO], generated from a series of experiments like the representative one shown here. The curve reaches an asymptote near 800 equivalents of NaClO per heme.

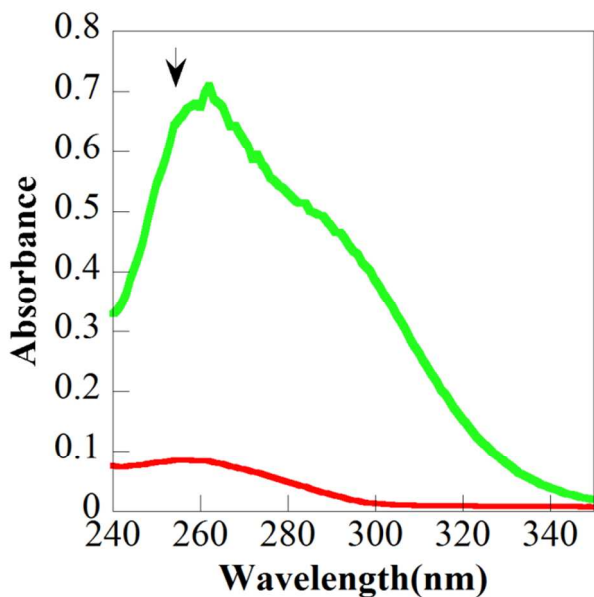
**Figure S6.**



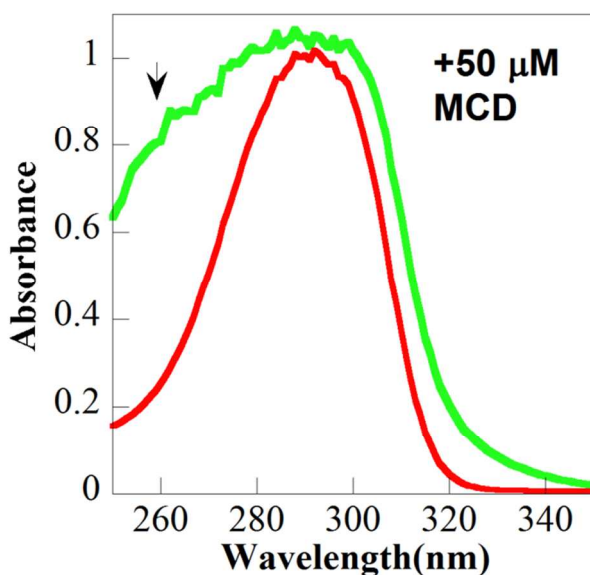
**Figure S6.** 50  $\mu$ L of 7.3  $\mu$ M heme-bound KpCld was added to 950  $\mu$ L 50 mM citrate-phosphate buffer, pH 6.0 or 8.0, in a UV/vis cuvette at room temperature. NaClO was added to final concentrations ranging from 0.15mM – 0.9mM. Immediately following each NaClO addition, the solution was mixed rapidly by pipetting up and the reaction monitored over time in scanning mode (250-700 nm) with scans every 6s. The reaction was monitored to completion, until the Soret band was eliminated and/or changes in the spectra ceased. First order rate constants ( $k_{obs}$ ) were fit to the resulting single exponential curves (A and B, pH 6 and 8 respectively) describing the change in the Soret band absorbance versus time. The values of  $k_{obs}$  were plotted versus [NaClO] to generate a second-order rate constant from the slope of the line (C).

Figure S7.

A.



B.



**Figure S7. Trappable HOCl is not formed in appreciable quantities during the *Da*Cld reaction.** The reaction between *Da*Cld and chlorite was monitored under conditions similar to those shown in the text in Figure 5A-C. Only the initial spectra ( $t_0$ , green) and final spectra ( $t_{30\text{min}}$ , red) are shown. **A.** 5mM  $\text{ClO}_2^-$  was added to 0.1 $\mu\text{M}$  of *Da*Cld in 50 mM potassium phosphate buffer, pH 7.4. 88% of the initially present  $\text{ClO}_2^-$  was degraded, according to iodometric titration of the end products. **B.** The reaction was run under the same conditions but in the presence of 50 mM MCD ( $\lambda_{\text{max}} \sim 290$  nm). While most of the chlorite ( $\lambda_{\text{max}} \sim 260$  nm) is eliminated under these conditions, little MCD is converted to its chlorinated product DCD, which has no absorbance at this wavelength.



**Table S1. Bacterial strains and plasmids used in this study**

Strain/ plasmid	Genotype/Features	Reference /Sources
<b>Strain</b>		
<i>Klebsiella pneumoniae</i> MGH 78578	Wild-type <i>K. pneumoniae</i> strain	ATCC
<b>KR3478</b>	<i>K. pneumoniae</i> MGH 78578 carrying pKOBEGApra	This study
<b>KR3444</b>	$\Delta$ cld <i>K. pneumoniae</i> MGH 78578 (Colony A)	This study
<b>KR3523</b>	$\Delta$ cld <i>K. pneumoniae</i> MGH 78578 (Colony B)	This study
<b>Plasmid</b>		
<b>pKOBEGApra</b>	Arabinose-inducible lambda Red expression plasmid; apramycin resistance	1
<b>pJTAG-hyg</b>	FRT- <i>hph</i> -FRT, hygromycin resistance cassette	2

1. **Chaveroche MK, Ghigo JM, d'Enfert C.** 2000. A rapid method for efficient gene replacement in the filamentous fungus *Aspergillus nidulans*. *Nucleic Acids Res* 28: E97.
2. **Zhang Y, Jiang X, Wang Y, Li G, Tian Y, Liu H, Ai F, Ma Y, Wang B, Ruan F, Rajakumar K.** 2014. Contribution of  $\beta$ -Lactamases and porin proteins OmpK35 and OmpK36 to carbapenem resistance in clinical isolates of KPC-2-producing *Klebsiella pneumoniae*. *Antimicrob Agents Chemother* 58:1214–1217.

**Table S2. Oligonucleotide primers used in this study.**

Primer number	Primer Name	Use/ target	Sequence (5'→3') <sup>a</sup>
-	GmF	FRT- <i>hph</i> -FRT	CGAATTAGCTTCAAAAGCGCTCTGA
-	GmR	FRT- <i>hph</i> -FRT	CGAATTGGGGATCTTGAAGTTCCT
-	EBGNHe-5	<i>gam, bet, exo</i>	CCCGCTAGCGAAAAGATGTTTCGTGAAGC
-	EBGh3-3	<i>gam, bet, exo</i>	GGGAAGCTTATTATCGTGAGGATGCGTCA
<b>P1</b>	cld-TS1-R	TS1	CCGTTATGTCATGCCTACCC
<b>P2</b>	cld-TS1-Fp/GmF	TS1	<u>TCAGAGCGCTTTTGAAGCTAATTCG</u> ATTCATCAGTTTCCTCTCAG
<b>P3</b>	cld-TS2-Rp/GmR	TS2	<u>AGGAACTTCAAGATCCCCAATTCG</u> TAGTATCAGGTTTA ACTGCG
<b>P4</b>	cld-TS2-F	TS2	CAACAACCTGGGTGGAAAACC
<b>P5</b>	cld-upstr-TS1-Rp	Screening	CAATTGGAACGGGGGCTTTG
<b>P6</b>	cld-downstr-TS2-Fp	Screening	GAACCTTCCTGGGTGACTGG
<b>P7</b>	cld-internal-F	<i>cld</i>	AAGTCGAAGGGTTCGCTCTC
<b>P8</b>	cld-internal-R	<i>cld</i>	TCGCGGGATAACGAGTAACG

<sup>a</sup> Underlined nucleotides corresponding to primers P2 and P3 are complementary to matching sequences of primers GmF and GmR, respectively.